



Materials and Energy Research Center  
MERC

Contents lists available at [ACERP](#)

Advanced Ceramics Progress

Journal Homepage: [www.acerp.ir](http://www.acerp.ir)



Advanced Ceramics Progress

## Original Research Article

# Investigation of the Substitution of Conventional Lead Oxide with a Lead Oxide-Silica Vitreous Composite in the Fabrication of Bi2223 Superconductor

Hossein Koohani <sup>1</sup>a, Mardali Yousefpour <sup>1</sup>b\*, Nastaran Riahi Nouri <sup>1</sup>c

<sup>a</sup> PhD Student, Department of Material Science, Semnan University, Semnan, Iran.

<sup>b</sup> Professor, Department of Material Science, Semnan University, Semnan, Iran.

<sup>c</sup> Assistant Professor, Department of Nonmetallic, Institute of Nirou Research, Tehran, Iran.

\* Corresponding Author Email: [myousefpor@semnan.ac.ir](mailto:myousefpor@semnan.ac.ir) (M. Yousefpour)

URL: [https://www.acerp.ir/article\\_239544.html](https://www.acerp.ir/article_239544.html)

## ARTICLE INFO

### Article History:

Received 09 September 2025

Received in revised form 11 November 2025

Accepted 02 January 2026

### Keywords:

Bi<sub>2223</sub> Bismuth-Based Superconductor.

Lead Oxide-Silica Vitreous Composite.

Additives.

Structural Analysis

## ABSTRACT

This research investigates the substitution of conventional lead oxide with a lead oxide-silica vitreous composite in the fabrication of Bi<sub>2223</sub> superconducting materials. The traditional Bi<sub>1.6</sub>Pb<sub>0.4</sub>Sr<sub>2</sub>Ca<sub>2</sub>Cu<sub>2</sub>O<sub>10+x</sub> formulation relies heavily on lead oxide to optimize phase formation and enhance superconducting properties. However, environmental and health concerns associated with lead oxide necessitate the development of alternative approaches. In this work, a 1:1 molar ratio of SiO<sub>2</sub>-PbO-based glassy matrix was employed as a partial replacement for pure PbO, maintaining 0.4 mole equivalents to achieve the target superconductor stoichiometry. The synthesized samples were characterized through X-ray diffraction analysis, scanning electron microscopy, and differential thermal analysis to evaluate structural characteristics and phase purity. Superconducting performance was assessed by measuring critical temperature and critical current density. Experimental results demonstrate that incorporation of the PbO-SiO<sub>2</sub> vitreous composite increases the Bi<sub>2223</sub> phase fraction from 76.8% (conventional PbO) to 89.7%, while enhancing the critical temperature (T<sub>c</sub>) by ~2.3 K. This suggests improved phase purity and superconducting performance, attributable to controlled Pb release and enhanced microstructural alignment. This lead-silica frit system presents notable benefits—such as lower toxicity and the flexibility to integrate functional additives like flux enhancers and mechanically stable layered structures—offering a more cost-effective and eco-friendly route for HTS synthesis.



<https://doi.org/10.30501/acp.2026.545163.1183>

## 1. INTRODUCTION

High-temperature superconductors (HTS), particularly Bi-based cuprates, have enabled transformative applications. Among the various HTS materials, the Bi-Sr-Ca-Cu-O (BSCCO) system, particularly the Bi<sub>2</sub>Sr<sub>2</sub>Ca<sub>2</sub>Cu<sub>3</sub>O<sub>10-δ</sub> (Bi<sub>2223</sub>) phase, has garnered significant attention due to its relatively high critical temperature (T<sub>c</sub> ≈ 110 K) and potential for practical applications in power transmission, magnetic resonance imaging, and magnetic levitation systems

([Sumitomo Electric Industries, 2025](#); [Tomita et al., 2011](#); [Tsukamoto et al., 2005](#); [Yao et al., 2021](#)).

The conventional fabrication process of Bi<sub>2223</sub> superconductors typically involves the use of lead oxide (PbO) as a key component in the precursor powder mixture. PbO serves multiple crucial functions in the synthesis process, including acting as a fluxing agent that facilitates the formation of liquid phases at elevated temperatures, promoting grain alignment, and enhancing the texturing of the superconducting grains ([Sumitomo](#)

Please cite this article as: Koohani, H., Yousefpour, M. & Riahi Nouri, N. (2025). Investigation of the Substitution of Conventional Lead Oxide with a Lead Oxide-Silica Vitreous Composite in the Fabrication of Bi<sub>2223</sub> Superconductor, *Advanced Ceramics Progress*, 11(2), 36-41. <https://doi.org/10.30501/acp.2026.545163.1183>

2423-7485/© 2025 The Author(s). Published by MERC.

This is an open access article under the CC BY license (<https://creativecommons.org/licenses/by/4.0/>).



[Electric Industries, 2025; Tomita et al., 2011](#)). However, the use of PbO presents several challenges, including environmental concerns due to lead toxicity, health hazards associated with lead exposure during processing, and the tendency for PbO to evaporate at high processing temperatures, leading to compositional inhomogeneity and reduced phase purity ([American Superconductor Corporation \(AMSC\); Kharissova et al., 2014; Koohani et al., 2025; Hayashi et al., 2020](#)).

In recent years, significant research efforts have been directed toward developing lead-free or reduced-lead alternatives for HTS fabrication. Various approaches have been explored, including the complete elimination of lead through modified processing routes and the partial substitution of PbO with other oxide systems. Among these alternatives, lead oxide-silica (PbO-SiO<sub>2</sub>) vitreous composites have emerged as promising candidates due to their unique properties. These composites combine the beneficial fluxing characteristics of PbO with the thermal stability and reduced volatility provided by the silica matrix.

The incorporation of silica into PbO-based systems offers several advantages. Silica acts as a viscosity modifier, potentially reducing PbO evaporation by increasing the melting point and viscosity of the fluxing medium. Additionally, the vitreous nature of PbO-SiO<sub>2</sub> composites can provide better chemical stability and controlled release of PbO during the sintering process. Studies on glass-ceramic systems have demonstrated that PbO-SiO<sub>2</sub> composites can maintain effective fluxing properties while exhibiting improved thermal and chemical stability compared to pure PbO.

The potential benefits of substituting conventional PbO with PbO-SiO<sub>2</sub> vitreous composites in Bi2223 fabrication include: (1) reduced lead volatility and associated environmental/health risks, (2) improved compositional control during processing, (3) enhanced microstructural development through modified liquid-phase sintering mechanisms, and (4) potential for lower processing temperatures or shorter processing times ([Herrera et al., 2004; 2002; 2002](#)).

However, the effectiveness of such substitution depends on various factors, including the composition of the vitreous composite, processing parameters, and the specific requirements of the Bi2223 formation mechanism.

Despite the theoretical advantages and preliminary studies on related systems, a systematic investigation of PbO-SiO<sub>2</sub> vitreous composite substitution in Bi2223 fabrication remains lacking in the literature. The complex interplay between the modified fluxing behavior, phase formation kinetics, and superconducting properties requires comprehensive analysis to determine the feasibility and optimization parameters for this approach.

This study aims to investigate the systematic substitution of conventional PbO with PbO-SiO<sub>2</sub> vitreous composites in the fabrication of Bi2223 superconductors.

The research will evaluate the effects of different composite compositions on phase formation, microstructural development, and superconducting properties, providing insights into the potential for developing more environmentally sustainable processing routes for high-temperature superconductors.

## 2. MATERIALS AND METHODS

### 2.1. Preparation of PbO-SiO<sub>2</sub> Vitreous Composite

The PbO-SiO<sub>2</sub> vitreous composite was synthesized through a conventional melt-quenching technique. High-purity PbO (Merck, CAS No 1317-36-8) and SiO<sub>2</sub> (Merck, CAS No 7631-86-9) powders were weighed according to stoichiometric calculations to achieve a 79 Wt.% PbO - 21 Wt.% SiO<sub>2</sub> composition (Eq. 1). The mixed powders were thoroughly homogenized using an agate mortar and pestle for 30 minutes to ensure uniform distribution.



The homogenized mixture was placed in an alumina crucible and heated in a muffle furnace at 500°C for one hour, as determined by preliminary dilatometry analysis (Figure 1), to remove any residual moisture and initiate the melting process. The temperature was then rapidly increased to 900°C and maintained for 30 minutes to ensure complete melting and homogenization of the components.

The molten mixture was subsequently quenched by pouring onto a preheated stainless-steel plate and subjected to rapid cooling to ambient temperature to form a glassy material. The resulting glass was ground using an agate mortar and sieved to obtain particles with sizes less than 10 μm for subsequent use as an additive.

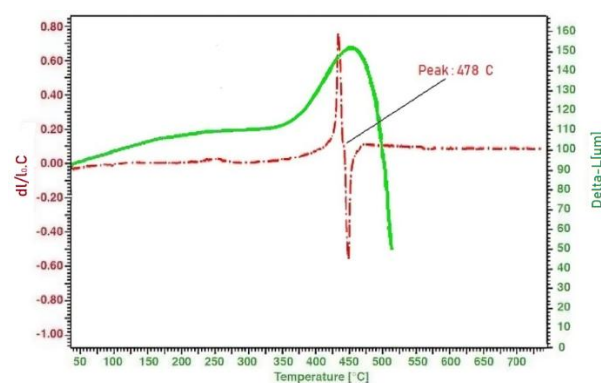


**Figure 1.** Dilatometry analysis of PbO-SiO<sub>2</sub> mixture during heating cycle

The amorphous nature of the prepared composite was confirmed through X-ray diffraction (XRD) analysis using Cu-Kα radiation (Figure 2), which showed the characteristic broad halo pattern indicative of glass formation without any detectable crystalline phases.

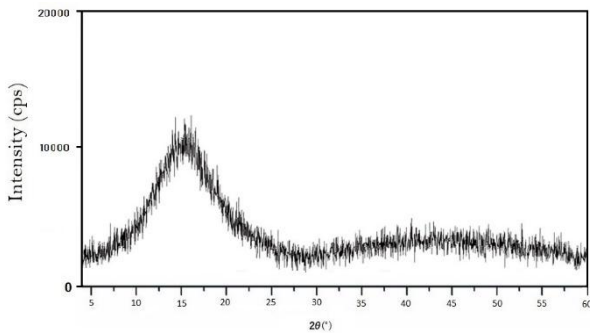


**Figure 2.** X-ray diffraction pattern confirming the amorphous nature of the prepared PbO-SiO<sub>2</sub> vitreous composite.

The 1:1 molar ( $\approx 79$  wt.% PbO–21 wt.% SiO<sub>2</sub>) composition lies in the metastable glass-forming region, where the eutectic-like behavior lowers the liquidus temperature ( $\sim 720$  °C vs.  $>850$  °C for pure PbO evaporation onset).

The glassy matrix suppresses PbO volatilization by increasing melt viscosity and forming a transient Pb<sub>2</sub>SiO<sub>4</sub> rich phase, which acts as a Pb reservoir during Bi2223 nucleation ( $\sim 820$ – $840$  °C).

A schematic phase-reaction pathway (Figure 3) illustrates PbO–SiO<sub>2</sub>  $\rightarrow$  Pb<sub>2</sub>SiO<sub>4</sub>  $\rightarrow$  PbO (controlled release)  $\rightarrow$  Bi2223 formation.

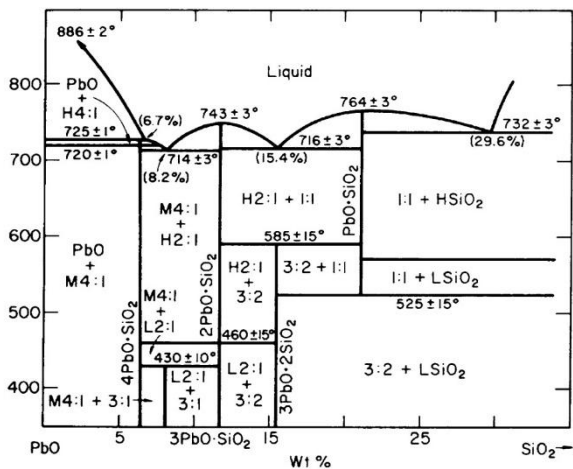


**Figure 3.** The PbO–SiO<sub>2</sub> binary phase diagram

## 2.2. Superconductor Sample Preparation

To evaluate the effectiveness of the PbO-SiO<sub>2</sub> vitreous composite as a substitute for conventional PbO in Bi2223 superconductor fabrication, three different sample compositions were prepared:

1. Reference sample (Sample A): Bi<sub>1.6</sub>Sr<sub>2</sub>Ca<sub>2</sub>Cu<sub>3</sub>O<sub>10+δ</sub> without any additional additives
2. Conventional sample (Sample B): Bi<sub>1.6</sub>Pb<sub>0.4</sub>Sr<sub>2</sub>Ca<sub>2</sub>Cu<sub>3</sub>O<sub>10+δ</sub> with PbO additive
3. Experimental sample (Sample C): Bi<sub>1.6</sub>(Pb, Si)<sub>0.4</sub>Sr<sub>2</sub>Ca<sub>2</sub>Cu<sub>3</sub>O<sub>10+δ</sub> with PbO-SiO<sub>2</sub> vitreous composite additive

For all samples, the required high-purity powders of Bi<sub>2</sub>O<sub>3</sub> (Sigma-Aldrich, CAS No 1304-76-3), PbO (Merck, CAS No 1317-36-8), SrCO<sub>3</sub> (Sigma-Aldrich, CAS No 1633-05-2), CaCO<sub>3</sub> (Merck, CAS No 471-34-1), and CuO (Merck, CAS No 1317-38-0) were weighed stoichiometrically according to the target composition Bi<sub>1.6</sub>Pb<sub>0.4</sub>Sr<sub>2</sub>Ca<sub>2</sub>Cu<sub>3</sub>O<sub>10+δ</sub>.

The raw materials were mixed thoroughly with their respective additive materials (either PbO or PbO-SiO<sub>2</sub> vitreous composite) in a polyethylene jar mill using zirconia balls and isopropanol as the milling medium. The milling process was conducted for 24 hours at 150 rpm to ensure homogeneous mixing and particle size reduction.

Following milling, the slurries were dried at 80°C for 12 hours to remove the isopropanol solvent. The dried powders were uniaxially pressed under equal pressure using a hydraulic press to form pellets with dimensions of 10 mm diameter and 2 mm thickness. All samples were subjected to identical pressing conditions to ensure comparability.

The pressed pellets were calcined at 820°C for 48 hours in air to promote the formation of the desired Bi2223 phase. After calcination, the samples were ground into fine powders using an agate mortar and pestle. Each sample was remixed in a laboratory jar mill for 4 hours to ensure uniform distribution of the additives.

The final powder mixtures were pressed again under identical conditions (200 MPa) to form pellets for sintering. To improve phase formation and densification, the pellets underwent two intermediate regrinding and repressing steps at 60 and 100 hours during their 140-hour sintering process in an air atmosphere at 839°C (Abdelhaleem et al., 2025; Abdullah et al., 2023; Garnier et al., 2001; Guilmeau et al., 2002; Kameli, 2006; Khaidir et al., 2025; Laliena et al., 2018; Polasecki, 2004; Taib et al., 2009; Verma et al., 2012; YangHao et al., 2023; Yavuz et al., 1998; ZhangShengnan et al., 2020).

## 3. RESULTS AND DISCUSSION

The Bi2223 superconductor is composed of alternating layers of BiO, Bi<sub>2</sub>O<sub>2</sub>, and CuO<sub>2</sub>, with its superconducting properties originating from the CuO<sub>2</sub> layers. The addition of various additives can influence the crystal structure and superconducting characteristics of the material. Initially, to compare the effects of the mentioned additives, X-ray analysis was performed on all samples.

The crystalline phases present in all samples were identified using X-ray diffraction (XRD) analysis with Cu-K $\alpha$  radiation ( $\lambda = 1.5418$  Å) at room temperature. The diffraction patterns were recorded in the  $2\theta$  range of 10° to 60° with a step size of 0.02° and counting time of 1 second per step.

Based on the X-ray analysis presented in Figure 3, only two phases, Bi2223 and Bi2212, were identified.

Therefore, calculations will proceed according to Eq. 2 as follows:

$$\text{Bi}[22(22(x-1)x)] (\%) = \frac{\Sigma[\text{Bi}22(x-1)x]}{\Sigma\text{Bi}2223+\Sigma\text{Bi}2212+\Sigma\text{Bi}2201} \times 100 \quad (2)$$

Based on Figure 4 and calculations using the Scherrer formula (Eq. 2), the relative percentages of different phases in the presented peaks can be determined (Table 1) (Koohani et al., 2025).

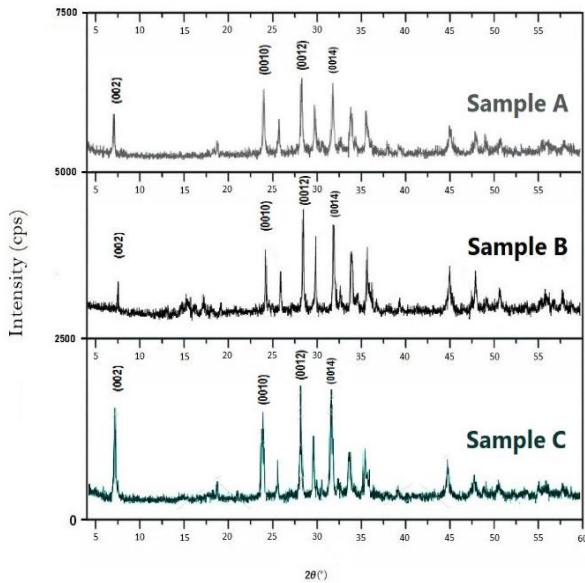


Figure 4. X-ray diffraction pattern confirming the various samples

Table 1. Different types of bi-based superconductor material phase ratios in samples.

Sample No	A	B	C
Bi2223 (%)	73.5	76.8	89.7
Bi2212 (%)	26.5	23.2	10.3

The analysis of X-ray results and calculated percentages indicates that the addition of vitreous composite not only increases the percentage of the Bi2223 phase but also leads to peak sharpness, which consequently promotes the growth of crystallite sizes. To further examine the outcomes derived from the X-ray analysis, the samples were studied using an electron microscope, and the findings are as follows:

The microstructural characteristics and phase distribution were examined using scanning electron microscopy (SEM) equipped with a particle distribution map for elemental analysis.

The samples were mounted in epoxy resin, polished using standard metallographic procedures, and carbon-coated prior to SEM examination (Obst et al., 2003; Popa et al., 2000; Singh et al., 2012).

Based on the results of the electron microscopy presented in Figure 5 and the particle distribution map, it

is evident that the additive particles are well distributed across all samples.

The superconducting particles predominantly exhibit a layered morphology, which is the dominant structural orientation. This layered orientation is notably more pronounced in the sample containing vitreous composite compared to other samples.

Finally, as shown in Figure 6, magnetic susceptibility analysis was conducted for all samples. The results indicate a favorable transition in the sample containing vitreous composite (Gömöry et al., 1997; Kang et al., 2011; Klepikova et al., 2021; Müller et al., 1991).

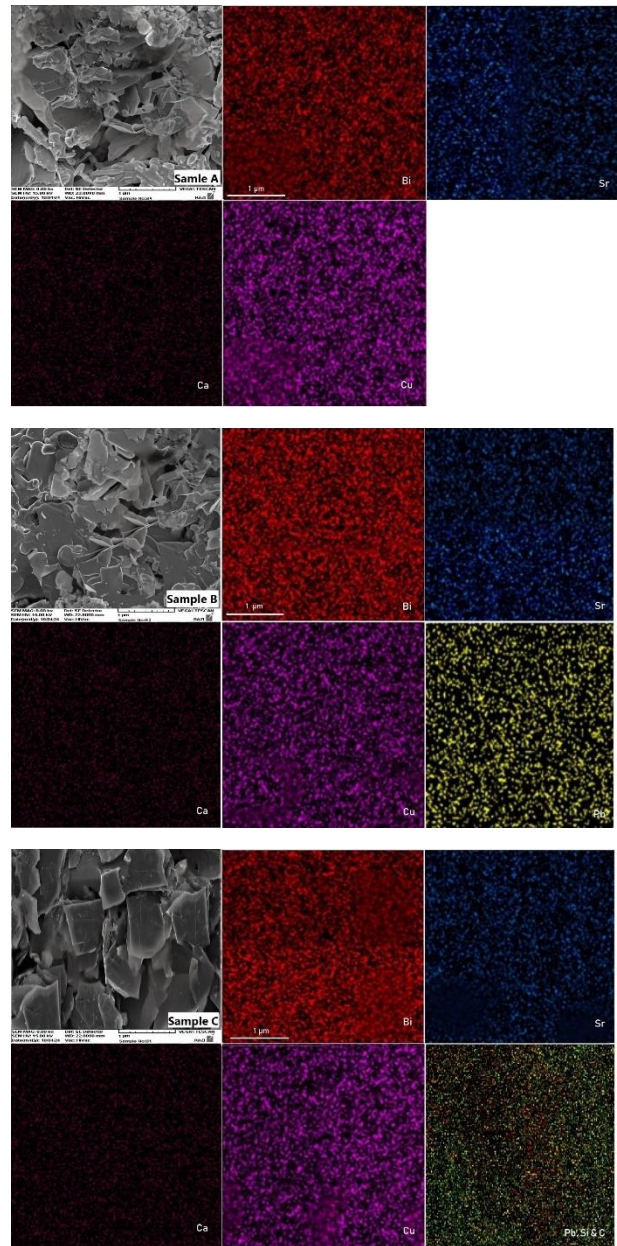
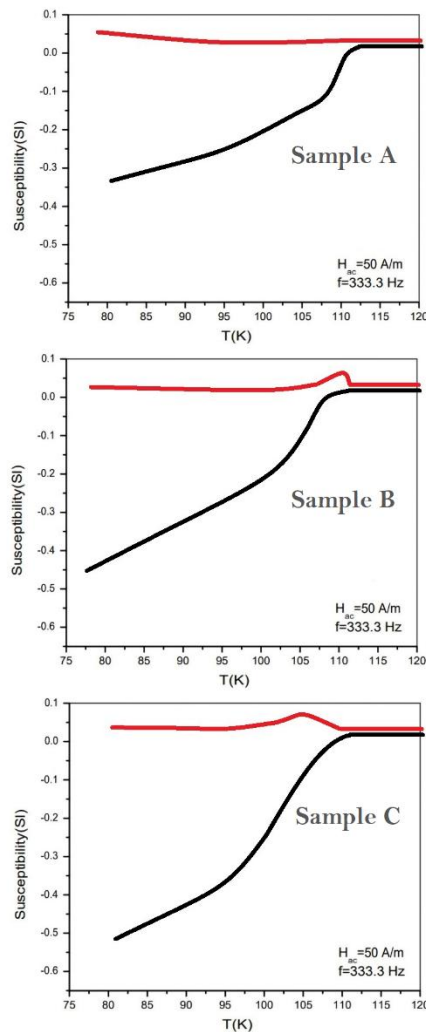


Figure 5. Scanning electron microscopy (SEM) pictures with a particle distribution map for elemental analysis.



**Figure 6.** Magnetic susceptibility analysis was conducted for all samples.

#### 4. CONCLUSION(S)

This study successfully demonstrates the feasibility of substituting conventional lead oxide with a lead oxide-silica vitreous composite in the fabrication of Bi2223 high-temperature superconductors. By incorporating a 1:1 molar ratio SiO<sub>2</sub>-PbO glassy matrix while maintaining the stoichiometric Pb content of 0.4 moles, the formation of the desired Bi2223 phase was effectively promoted, as confirmed by X-ray diffraction, scanning electron microscopy, and differential thermal analysis. Notably, samples prepared with the vitreous composite exhibited an enhanced critical temperature ( $T_c$ ) compared to those synthesized using pure PbO, indicating improved superconducting properties. The homogeneous dispersion of Pb provided by the glassy matrix likely facilitates better phase development and microstructural uniformity. Importantly, this approach significantly reduces the environmental and health hazards associated with handling toxic PbO powders, offering a safer and more sustainable processing route. Furthermore, the

versatility of the glassy system allows for the potential integration of functional additives to improve flux pinning and mechanical integrity. Collectively, the PbO-SiO<sub>2</sub> vitreous composite emerges as a compelling alternative to conventional PbO—simultaneously enhancing superconducting performance, improving process safety, and aligning with green manufacturing principles. This strategy not only mitigates lead-related environmental and health risks but also opens avenues for multifunctional additive integration, thus advancing the scalability and sustainability of Bi2223 superconductor production.

Future work will systematically vary the PbO:SiO<sub>2</sub> ratio (60:40 to 90:10) to identify the optimum window for Bi2223 phase yield and  $T_c$ .

#### ACKNOWLEDGEMENTS

Our sincere gratitude goes out to Semnan University and the NRI Institute for their invaluable support and resources during this research. Their commitment to fostering academic excellence and providing a conducive environment for scientific inquiry has greatly contributed to the success of this work. We appreciate the collaboration and assistance offered by the faculty and staff, which has been instrumental in the completion of this study. Thank you for your unwavering support

#### REFERENCES

1. Abdelhaleem, S., Alziyadi, M. O., & Alruwaili, A. (2025). BSCCO high  $T_c$ -superconductor materials: Strategies toward critical current density enhancement and future opportunities. *Appl. Phys. A*, *131*, Article 151. <https://doi.org/10.1007/s00339-025-08262-y>
2. Abdullah, S. N. (2023). Microstructure and superconducting properties of Bi2223 synthesized via co-precipitation method: Effects of graphene nanoparticle addition. *Nanomaterials*, *13*(15), 2197. <https://doi.org/10.3390/nano13152197>
3. American Superconductor Corporation (AMSC). (n.d.). <https://www.amsc.com/>
4. Garnier, V., Monot-Laffez, I., & Desgardin, G. (2001). Optimization of sintering conditions on the Bi-2223 formation and grain size. *Mater. Sci. Eng. B*, *83*, 48–54. [https://doi.org/10.1016/S0921-5107\(00\)00665-6](https://doi.org/10.1016/S0921-5107(00)00665-6)
5. Gömöry, F. (1997). Characterization of high-temperature superconductors by AC susceptibility measurements. *Supercond. Sci. Technol.*, *10*, 523. <https://doi.org/10.1088/0953-2048/10/8/001>
6. Guilmeau, E., Chateigner, D., & Noudem, J. G. (2002). Sinter-forging of strongly textured Bi2223 discs with large  $J_c$ : Nucleation and growth of Bi2223 from Bi2212 crystallites. *Supercond. Sci. Technol.*, *15*, 1436–1444. <http://stacks.iop.org/SUST/15/1436>
7. Hayashi, K. (2020). Commercialization of Bi-2223 superconducting wires and their applications. *SEI Tech. Rev.*, (91), 68-74. <https://global-sei.com/technology/tr/bn91/pdf/E91-12.pdf>
8. Herrera, M. U., & Sarmago, R. V. (2002). Synthesis of Pb-doped Bi2223 from Pb-doped Bi2212, Ca<sub>2</sub>CuO<sub>3</sub>, and CuO above the glass transition temperature of Bi2212. *Sci. Diliman*, *14*(2), 51–58. <https://scispace.com/pdf/synthesis-of-pb-doped-bi-2223-from-pb-doped-bi-2212-ca2cuo3-5687se4k2q.pdf>

9. Herrera, M. U., & Sarmago, R. V. (2002). Synthesis of Pb-free Bi2223 from Bi2212 using partial melting. *Philipp. Eng. J.*, 23(2), 35-48. <https://scispace.com/pdf/synthesis-of-pb-free-bi-2223-from-bi-2212-using-partial-320849dxmu.pdf>
10. Herrera, M. U., & Sarmago, R. V. (2004). Synthesis of Pb-doped Bi-2223 from Pb-doped Bi-2212 via partial melting. *Ceram. Int.*, 30(7), 1611-1614. <https://doi.org/10.1016/j.ceramint.2003.12.186>
11. Kameli, P. (2006). The effect of sintering temperature on the intergranular properties of Bi2223 superconductors. *Solid State Commun.*, 137(1-2), 30-35. <https://doi.org/10.1016/j.ssc.2005.10.026>
12. Kang, M., Kim, Y., Lee, H., Cha, G., & Ryu, K. (2011). Magnetic field and critical current of a BSCCO HTS magnet at various aspect ratios. *IEEE Trans. Appl. Supercond.*, 21(3), 2271. <https://doi.org/10.1109/TASC.2010.2086422>
13. Khaidir, R. E. M., Kamarudin, A. N., Awang Kechik, M. M., Kien, C. S., Pah, L. K., Shabdin, M. K., ... Shaari, A. H. (2025). Influence of sintering temperature on phase formation and superconducting properties of Bi2Sr2CaCu2O8+ $\delta$  via thermal treatment method. *J. Mater. Sci. Radiat.*, 1(1), 1-6. <https://journals.balaipublikasi.id/index.php/jmsr/article/view/359>
14. Kharissova, O. V., Kopnin, E. M., & Kopnin, E. M. (2014). Recent advances on bismuth-based 2223 and 2212 superconductors: Synthesis, chemical properties, and principal applications. *Crit. Rev. Solid State Mater. Sci.*, 39(4). <https://doi.org/10.1080/10408436.2013.836073>
15. Klepikova, A. S., Charikova, T. B., & Popov, M. R. (2021). Magnetic susceptibility anisotropy of electron overdoped high temperature superconductor Nd<sub>2-x</sub>Ce<sub>x</sub>CuO<sub>4</sub>. *J. Phys. Chem. Solids*, 148, 109770. <https://doi.org/10.1016/j.jpcs.2020.109770>
16. Koohani, H., Yousefpour, M., & Riahi, N. (2025). Investigation of the effect of varied graphene oxide additions on Bi2223 superconductor properties. *Phys. B*, Article 417114. <https://doi.org/10.1016/j.physb.2025.417114>
17. Laliena, C., Amaveda, H., Özçelik, B., & Martínez, E. (2018). Continuous processing of Bi2Sr2CaCu2O8+ $\delta$  precursor powders. *Ceram. Int.*, 44(12), 14865-14872. <https://doi.org/10.1016/j.ceramint.2018.05.120>
18. Müller, K. H., Nikolo, M., Savvides, N., & Driver, R. (1991). Ac susceptibility of high-temperature ceramic superconductors: Critical state and creep at grain boundaries and in grains. In K. Kajimura & H. Hayakawa (Eds.), *Adv. Supercond. III* (pp. 130). Springer. [https://doi.org/10.1007/978-4-431-68141-0\\_130](https://doi.org/10.1007/978-4-431-68141-0_130)
19. Obst, B., Nast, R., & Schlachter, S. (2003). Application of electron backscatter diffraction in the SEM to textural problems of coated high-temperature superconductors. *Int. J. Mater. Res.*, 94(5), 580-586. <https://doi.org/10.1515/ijmr-2003-0101>
20. Polasek, A. (2004). Phase relations study on the melting and crystallization regions of the Bi2223 high temperature superconductor. *Mat. Res.*, 7(3). <https://doi.org/10.1590/S1516-14392004000300005>
21. Popa, M., Calderon-Moreno, J., & Zaharescu, M. (2000). TEM and SEM studies on the formation of superconducting phases in the Bi-based system. *J. Eur. Ceram. Soc.*, 20(16), 2773-2778. [https://doi.org/10.1016/S0955-2219\(00\)00225-9](https://doi.org/10.1016/S0955-2219(00)00225-9)
22. Singh, S. K., Sharma, D., & Husain, M. (2012). Exploring the superconductors with scanning electron microscopy (SEM). In *Scanning Electron Microscopy*. IntechOpen. <https://doi.org/10.5772/35675>
23. Sumitomo Electric Industries, Ltd. (n.d.). <https://global-sei.com/>
24. Taib, H. (2009). *Synthesis and electrophoretic deposition of tin oxide (SnO<sub>2</sub>)* [Doctoral dissertation, University of New South Wales]. ResearchGate. <https://www.researchgate.net/publication/277832420>
25. Tomita, M. (2011). Next generation of prototype direct current superconducting cable for railway system. *J. Appl. Phys.*, 109, 063909. <https://doi.org/10.1063/1.3553843>
26. Tsukamoto, O. (2005). Roads for HTS power applications to go into the real world: Cost issues and technical issues. *Cryogenics*, 45, 3-10. <https://doi.org/10.1016/j.cryogenics.2004.06.008>
27. Verma, I. (2012). Synthesis and magnetic properties of (Bi,Pb)2Sr2Ca2Cu3O10+ $\delta$  superconductor. *J. Supercond. Nov. Magn.*, 25, 785-789. <https://link.springer.com/article/10.1007/s10948-011-1339-6>
28. YangHao, B., Qingbin, Q., & Xiao, P. (2023). Preparation of high-performance high temperature superconducting Bi-2212 wires by the spray pyrolysis powder. *J. Mater. Sci. Mater. Electron.*, 34(23). <https://doi.org/10.1007/s10854-023-11072-8>
29. Yao, C., & Ma, Y. (2021). Superconducting materials: Challenges and opportunities for large-scale applications. *iScience*, 24, 102541. <https://doi.org/10.1016/j.isci.2021.102541>
30. Yavuz, M., & Vance, H. M. (1998). Effect of ball milling materials and methods on powder processing of Bi2223 superconductors. *Supercond. Sci. Technol.*, 11(10), 1153-1159. <https://doi.org/10.1088/0953-2048/11/10/056>
31. Zhang, S., Shao, B., & Ma, S. (2020). Influence of calcination atmosphere on the phase evolution mechanism of Bi-2223 high temperature superconductor. *J. Mater. Sci. Mater. Electron.*, 31(1). <https://doi.org/10.1007/s10854-020-03779-9>